

Manipulation of gray-ring dark solitons in a two-component Bose gas with tunable soft-core interactions

Qiu-Ling He(何秋玲), Lin-Xue Wang(王林雪), Rui Jin(金瑞), Fang Wang(王芳), Ya-Jun Wang(王雅君), and Xiao-Fei Zhang(张晓斐)

Citation: Chin. Phys. B, 2025, 34 (**10**): 100306. DOI: 10.1088/1674-1056/addcbf
http://cpb.iphy.ac.cn; http://iopscience.iop.org/cpb

What follows is a list of articles you may be interested in

Manipulation of gray-ring dark solitons in a two-component Bose gas with tunable soft-core interactions

Qiu-Ling He(何秋玲), Lin-Xue Wang(王林雪), Rui Jin(金瑞), Fang Wang(王芳), Ya-Jun Wang(王雅君), and Xiao-Fei Zhang(张晓斐)
Chin. Phys. B, 2025, 34 (**10**): 100306. DOI: 10.1088/1674-1056/addcbf

Ground state of SU(3) spin-orbit coupled soft-core Bose gas

Jia Liu(刘佳), Jing Feng(冯婧), Ya-Jun Wang(王雅君), Xiao-Fei Zhang(张晓斐), and Xue-Ying Yang(杨雪滢)
Chin. Phys. B, 2025, 34 (**6**): 060301. DOI: 10.1088/1674-1056/adc36b

Effects of drive imbalance on the particle emission from a Bose-Einstein condensate in a one-dimensional lattice

Long-Quan Lai(赖龙泉) and Zhao Li(李照)
Chin. Phys. B, 2024, 33 (**3**): 030308. DOI: 10.1088/1674-1056/ad1172

Dynamical nonlinear excitations induced by interaction quench in a two-dimensional box-trapped Bose-Einstein condensate

Zhen-Xia Niu(牛真霞) and Chao Gao(高超)
Chin. Phys. B, 2024, 33 (**2**): 020314. DOI: 10.1088/1674-1056/ad1179

Effects of drive imbalance on the particle emission from a Bose-Einstein condensate in a one-dimensional lattice

Long-Quan Lai(赖龙泉) and Zhao Li(李照)
Chin. Phys. B, 2024, 33 (**3**): 030308. DOI: 10.1088/1674-1056/ad1172

Manipulation of gray-ring dark solitons in a two-component Bose gas with tunable soft-core interactions

Qiu-Ling He(何秋玲)[1], Lin-Xue Wang(王林雪)[1], Rui Jin(金瑞)[1], Fang Wang(王芳)[1], Ya-Jun Wang(王雅君)[2], and Xiao-Fei Zhang(张晓斐)[1,†]

[1] *School of Physics and Information Science, Shaanxi University of Science and Technology, Xi'an* 710021, *China*
[2] *Department of Basic Sciences, Air Force Engineering University, Xi'an* 710051, *China*

(Received 21 March 2025; revised manuscript received 6 May 2025; accepted manuscript online 23 May 2025)

We explore the manipulation of gray-ring dark solitons in a two-component Bose gas with tunable soft-core interactions through numerical simulations of the time-dependent Gross–Pitaevskii equation. Our results demonstrate that the lifetime of gray solitons with periodically modulated soft-core interactions significantly depends on their initial depth. Specifically, shallower initial depths lead to longer lifetimes when exceeding a critical depth threshold. Furthermore, the soliton depth also governs the number and dynamic of vortex pairs resulting from the collapse of the ring dark soliton. These depth-dependent topological transformations open new perspectives for quantum manipulation.

Keywords: Bose–Einstein condensate, Rydberg interaction, ring dark solitons

PACS: 03.75.Hh, 67.85.–d, 67.85.De, 75.10.–b

DOI: 10.1088/1674-1056/addcbf **CSTR:** 32038.14.CPB.addcbf

1. Introduction

In recent years, significant breakthroughs have been made in the study of the control mechanisms of nonlinear excited states in ultracold quantum systems,[1–4] among which Bose–Einstein condensates (BECs) based on Rydberg interactions exhibit unique dynamic characteristics.[5–8] As a typical localized wave solution, the soliton's ability to maintain stable propagation of its waveform has been systematically explained through the nonlinear Schrödinger equation in uniform BEC systems, revealing the rich physical implications of the nonlinear Schrödinger equation.[9–13] However, the soliton dynamics in traditional short-range interaction systems are limited by the inability to tune interaction strength, making it difficult to explore nonequilibrium behaviors under complex geometric configurations.[14–17] The stability of solitons in ring potential fields is often difficult to maintain due to the dynamic instability induced by quantum fluctuations. This issue has prompted researchers to shift towards new quantum systems with higher degrees of control freedom.[18–20]

Crucially, the implementation of Rydberg-dressed interactions has emerged as a critical pathway to realizing soft-core interactions, which differ fundamentally from conventional short-range contact interactions. Unlike the hard-core interactions in traditional systems, soft-core interactions exhibit tunable nonlocal characteristics, enabling unprecedented control over soliton dynamics. Rydberg interacting Bose gases, due to their unique nonlocal interaction characteristics, have become an important platform for studying the dynamics of topological excitation states in quantum fluids.[21–24] Experiments have confirmed that electromagnetic field control can realize long-range interactions on the micrometer scale.[25–27] This mechanism not only reshapes the collective excitation spectrum of the system but also provides a unique advantage for the precise control of the dynamics of nonlinear structures such as solitons and vortices.[28,29]

Previous experiments have successfully observed a series of nonlinear phenomena in BEC, including dark solitons (referred to as black solitons when the minimum density at their center is zero, and gray solitons when the minimum density is non-zero),[30] bright solitons,[31] and vortices.[32] These discoveries have made the study of matter-wave solitons one of the research hotspots in the field of BECs.[33] Notably, gray-ring dark solitons (RDSs), as topological excitation states carrying nontrivial phase structures, exhibit nontrivial phase transition properties, with substantial research already conducted in short-range interaction systems.[34,35] Research on black solitons is also extensive; however, the impact of the initial depth of RDSs on system dynamics in Rydberg systems remains an important issue that requires further investigation.[36–38] The gray RDSs exhibits a unique angular momentum-topological coupling effect in a rotationally symmetric potential due to its closed phase boundary conditions.[39] Theoretical studies suggest that in conventional short-range interaction systems, the lifetime of solitons is typically limited by dynamic instability induced by quantum fluctuations.[40,41] However, Rydberg interactions, by introducing spatially correlated nonlinear potential barriers, can effectively suppress the radial dispersion of solitons and enhance

†Corresponding author. E-mail: xfzhang@sust.edu.cn

© 2025 Chinese Physical Society and IOP Publishing Ltd. All rights, including for text and data mining, AI training, and similar technologies, are reserved.

their topological stability.[42–45] Recent experimental studies show that the Rydberg dressing technique can dynamically control the shape of the interaction potential, enabling control over the soliton's trajectory.[46] Nevertheless, most existing research focuses on the propagation characteristics of solitons in homogeneous or linear potential fields.[47,48] There is relatively little research on the dynamics of gray RDSs evolution under ring-shaped confinement and non-local Rydberg interactions, and further exploration is needed.

The main purpose of this work is to study the effect of initial depth on the dynamics and lifetime of gray RDSs. The organizational structure of this work is as follows. In Section 2, we describe the theoretical model of the system. In Section 3, we discuss in detail the effect of initial depth on the dynamics of gray RDSs and the effect on the solitons' lifetimes. Finally, the main achievements of this paper are summarized in the Section 4.

2. Theoretical model

We study a two-component BEC with both contact interactions and nonlocal Rydberg interactions. Within the mean-field approximation, the dynamics of the system are described by the following coupled Gross–Pitaevskii (GP) equations[20,49,50]

$$\begin{aligned}
\mathrm{i}\hbar\frac{\partial\Psi_1}{\partial t} &= \Big(-\frac{\hbar^2\nabla^2}{2m}+V(\boldsymbol{r},z)+G_{11}|\Psi_1|^2 \\
&\quad +G_{12}|\Psi_2|^2+U_{11}|\Psi_1|^2+U_{12}|\Psi_2|^2\Big)\Psi_1, \\
\mathrm{i}\hbar\frac{\partial\Psi_2}{\partial t} &= \Big(-\frac{\hbar^2\nabla^2}{2m}+V(\boldsymbol{r},z)+G_{22}|\Psi_1|^2 \\
&\quad +G_{21}|\Psi_2|^2+U_{22}|\Psi_2|^2+U_{21}|\Psi_1|^2\Big)\Psi_2, \qquad (1)
\end{aligned}$$

where Ψ_i is the wave function of the i-th component, which must satisfy the following normalization condition $N_i = \int|\Psi_i|^2\mathrm{d}\boldsymbol{r}\,\mathrm{d}z$. Here $\nabla^2 = \partial^2/\partial x^2+\partial^2/\partial y^2+\partial^2/\partial z^2$ and m denotes the mass of the atoms, $G_{ii} = 4\pi a_{ii}\hbar^2/m$ and $G_{ij} = 4\pi a_{ij}\hbar^2/m$ represents the intra- and inter-component contact interactions, which are related to s-wave scattering lengths a_{ii} and a_{ij}, and can be tuned using Feshbach resonance techniques. $U_{ii}(\boldsymbol{r},\boldsymbol{r}') = \int[C_6^{ii}/(R_\mathrm{c}^6+|\boldsymbol{r}-\boldsymbol{r}'|^6)]\,\mathrm{d}\boldsymbol{r}'$, and $U_{ij}(\boldsymbol{r},\boldsymbol{r}') = \int[C_6^{ij}/(R_\mathrm{c}^6+|\boldsymbol{r}-\boldsymbol{r}'|^6)]\,\mathrm{d}\boldsymbol{r}'$ represents the intra- and inter-component nonlocal Rydberg interactions, which R_c, C_6^{ii}, and C_6^{ij} represent the Rydberg blockade radius and the strengths of the nonlocal Rydberg interactions, respectively. The external potential is a harmonic potential, denoted by $V(\boldsymbol{r},z) = m(\omega_\mathrm{r}^2\boldsymbol{r}^2+\omega_z^2z^2)/2$, where ω_r and ω_z represent the radial and axial constraint frequencies, respectively. Next, we explore the quasi-two-dimensional (Q2D) system that can be realized by applying a very strong confinement along the z axis, i.e., when $\hbar\omega_z$ is much larger than any other energy scale, the order parameter can be separated into the following form: $\Psi_i(\boldsymbol{r}) = Z(z)\psi_i(x,y)$, where $Z(z) = \mathrm{e}^{-z^2/2a_z^2}/(\pi a_z^2)^{1/4}$ is the ground state of a harmonic oscillator with frequency ω_z, and $a_z = [\hbar/(m\omega_z)]^{1/2}$. After integrating over the axial coordinates, the following dimensionless coupled GP equations can be used to describe the radial wave function:[51,52]

$$\begin{aligned}
\mathrm{i}\frac{\partial\psi_1}{\partial t} &= \Big(-\frac{1}{2}\nabla^2+\frac{1}{2}\Omega^2r^2+g_{11}|\psi_1|^2 \\
&\quad +g_{12}|\psi_2|^2+A_{11}|\psi_1|^2+A_{12}|\psi_2|^2\Big)\psi_1, \\
\mathrm{i}\frac{\partial\psi_2}{\partial t} &= \Big(-\frac{1}{2}\nabla^2+\frac{1}{2}\Omega^2r^2+g_{22}|\psi_2|^2 \\
&\quad +g_{21}|\psi_1|^2+A_{22}|\psi_2|^2+A_{21}|\psi_1|^2\Big)\psi_2, \qquad (2)
\end{aligned}$$

where the aspect ratio of the potential well is $\Omega = \omega_\mathrm{r}/\omega_z$, and the units of length and time are $a_z = \sqrt{\hbar/m\omega_z}$ and $1/\omega_z$, respectively. The Q2D contact interactions are re-expressed using $g_{ii} = 2\sqrt{2\pi}\hbar^2a_{ii}/(ma_z)$, $g_{ij} = 2\sqrt{2\pi}\hbar^2a_{ij}/(ma_z)$, and the Q2D Rydberg interactions are re-expressed using $C_6^{(ii)}/R_\mathrm{c}^4$ and $C_6^{(ij)}/R_\mathrm{c}^4$. In the following content, the nonlocal Rydberg interactions are simplified to A_{ii} and A_{ij}. We mainly discuss the cases of $A_{11} = A_{22} \equiv A$, $g_{11} = g_{22} = g_{12} = g_{21} \equiv 1$, which are closely related to the ^{87}Rb system.

As mentioned earlier, the concept of RDS was first introduced in the field of nonlinear optics and was later applied to BEC systems. We choose an initial state in which each component contains an RDS with an initial radius, and replace the exact solution of the RDS with an appropriate approximate solution

$$\begin{aligned}
\psi_i(x,y,0) &= \Big(1-\frac{\Omega^2r^2}{4}\Big) \\
&\quad \times\Big[\cos\phi_i(0)\tanh Z(r_1)+\mathrm{i}\sin\phi_i(0)\Big], \qquad (3)
\end{aligned}$$

where $\cos\phi_i(0)$ is proportional to the depth of the input soliton, and $e_\mathrm{c} = 0$ is the eccentricity of the ring, and $Z(r_1) = (r_1-R_{i0})\cos\phi_i(0)$ with $r_1 = \sqrt{(1-e_\mathrm{c}^2)x^2+y^2}$. The initial radius is represented by R_{i0}, where $R_{10} = 27.9$, $R_{20} = 28.9$, and $\Delta R = R_{20}-R_{10}$ denotes the difference in radius. We set it as $\Delta R = 1$ in our work. To achieve periodic modulation of the Rydberg interactions, we can vary the intra- and inter-component nonlocal Rydberg interactions. We set the periodic modulation inter-component nonlocal Rydberg interactions as $A_{ij}(t) = 0.08+k\sin(\omega t)$. The modulation frequency is ω, so the modulation period is $2\pi/\omega$, and k is the modulation amplitude, satisfying $0 \le k \le 1$. Here, we set $\omega = \Omega = 0.028$ and $k = 0.02$. Meanwhile we fix the intra-component Rydberg interaction $A_{ii} = 0.08$ to explore the impact of different initial depths on the soliton lifetime and dynamics.

In the subsequent numerical simulation, we used alternating direction implicit method and time-split Fourier spectrum

method respectively, and cross-checked the obtained results, and found that the results were in good agreement.[53,54]

3. Results and discussion

In what follows we will perform a detailed study of the effects of the initial depth on the lifetime and dynamics of gray RDSs in a BEC system with tunable Rydberg interactions, where the lifetime of gray RDSs refers to the time interval between the start and the time point when broken sets in. Through numerical simulations, we find that the lifetime of the solitons increase with decreasing depth when exceeding a critical depth threshold. Figure 1 shows the moment of RDSs broken of component-1 at different initial depths $\cos\phi_1(0) = \cos\phi_2(0) = \cos\phi(0) = 0.95, 0.75, 0.63$, while reflecting the lifetime of the gray RDSs. This indicates that shallow solitons exhibit stronger dynamical stability, and this finding provides an important theoretical basis for achieving long-lived topological excitations through Rydberg dressing techniques. Next, we discuss in detail the dynamics of gray RDSs at these three different initial depths with periodically modulated Rydberg interactions.

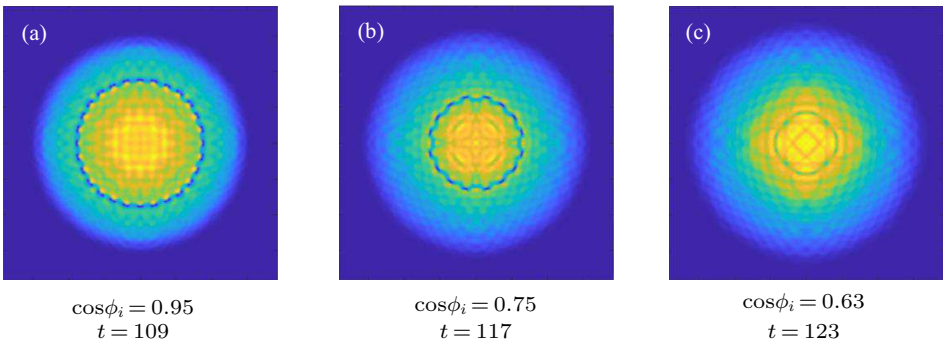


Fig. 1. The lifetime diagram of the gray RDSs at different initial depths. The eccentricity is $e_c = 0$, the initial radii are $R_{10} = 27.9$ and $R_{20} = 28.9$, the modulation amplitude is $k = 0.02$, the modulation frequency is $\omega = 0.028$, and the aspect ratio of the harmonic trap is $\Omega = \omega = 0.028$. The intra-component Rydberg interaction in the components is $A_{11} = A_{22} = A = 0.08$. The field of view is 150×150 in dimensionless units.

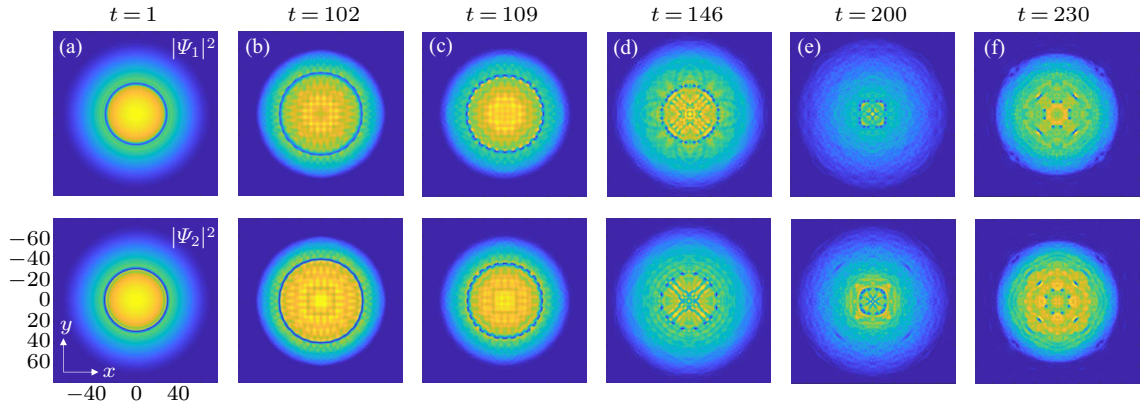


Fig. 2. The typical time evolution diagram of the gray RDSs with an initial depth of $\cos\phi_1(0) = \cos\phi_2(0) = 0.95$. (a) $t = 1$, (b) $t = 102$, (c) $t = 109$, (d) $t = 146$, (e) $t = 200$, and (f) $t = 230$. The top row is for component 1, while the bottom row is for component 2. The eccentricity is $e_c = 0$, the initial radii are $R_{10} = 27.9$ and $R_{20} = 28.9$, the modulation amplitude is $k = 0.02$, the modulation frequency is $\omega = 0.028$, and the aspect ratio of the harmonic trap is $\Omega = \omega = 0.028$. The intra-component Rydberg interaction in the components is $A_{11} = A_{22} = A = 0.08$. The field of view is 150×150 in dimensionless units.

Figures 2 and 3 illustrate the typical time evolution of the gray RDSs with the initial depth of $\cos\phi_1(0) = \cos\phi_2(0) = 0.95$ for the case with the deeper initial depth, where the top row is for component 1 and the bottom one is for component 2. Here only discussed the detailed dynamics of component-1, since component-2 has similar dynamics behavior, but with different time scales. Starting from the initial moment, the gray RDSs exhibits oscillations outward, and then gradually contracts. Over time, the soliton undergoes significant deformation due to snake instability, as shown in Fig. 2(b) for $t = 102$. With instability further develops, the symmetry of the deformed circular is soon broken, which eventually forms a vortex necklace structure composed of 28 pairs of vortex and antivortex, as shown in Fig. 2(c) for $t = 109$. As the evolution progresses, some vortex pairs begin to move toward the center of the condensate, with 4 pairs moving each time, and after gathering at the center, they expand outward along the x direction. More notably, we observed that vortex pairs annihilated in symmetric groups of four during their motion, governed by collective decay dynamics tied to their spatial and topological order.[55] As predicted by symmetry-breaking theories, the number of vortex pairs of the vortex chain is reduced to 16 pairs, as shown in Fig. 2(d) for $t = 146$. When the time reaches $t = 200$, as shown in Fig. 2(e), 4 pairs of vortices meet at the

center of the condensate, and the other 8 pairs are arranged from a circle shape to a square structure. Although the rectangular vortex necklace-like structure is likely due to effects of periodic boundary conditions, such the pattern of vortex chain is markedly different from previous studies.[20,56,57]

After that, the dynamics of the vortices can be divided into three layers of concentric ring trajectories which are the central, the middle, and the outermost layer, as shown in Fig. 2(f) for $t = 230$. The vortex–antivortex pairs in the central layer move toward each other due to mutual attraction, the vortex pairs in the middle and outer layers will undergo complex dynamical behavior of splitting and recombination. With time going on, the quartets of vortex and antivortex in the middle layer move away each other while pairs toward the periphery of condensate in the x shape direction. The vortices recombine with another antivortices to form a new topological defect pairs, and then move inward to the center of the condensate in the + shape direction, as shown in Figs. 3(a)–3(e). The 4 vortex pairs split into vortices and antivortices in the outermost layer while moving in opposite directions along the edge, as shown in Fig. 3(a) for $t = 285$. In this process, the outermost vortex (antivortex) and the antivortex (vortex) of the middle layer approach each other, as shown in Fig. 3(c) for $t = 490$. The outermost vortices are the first to be annihilated, and the other vortex pairs repeat similar previous motion until annihilated, as shown in Figs. 3(e)–3(f).

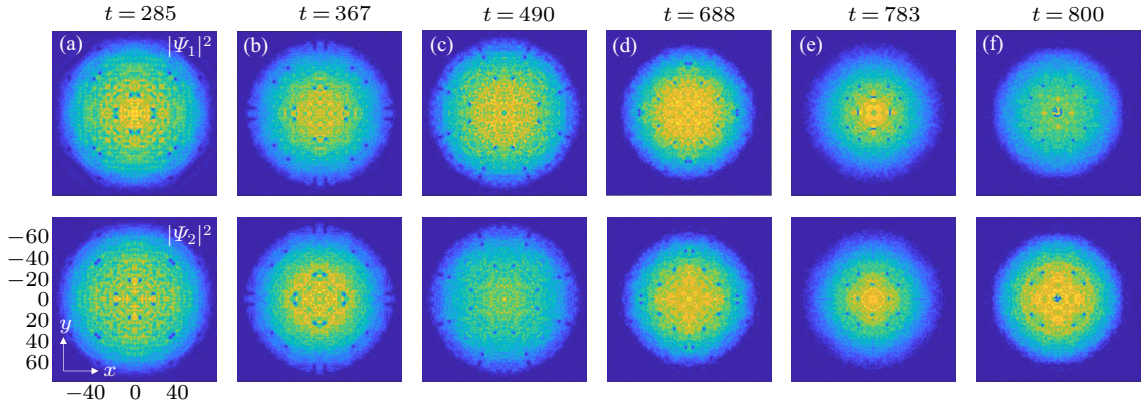


Fig. 3. The typical time evolution diagram of the gray RDSs with an initial depth of $\cos\phi_1(0) = \cos\phi_2(0) = 0.95$. (a) $t = 285$, (b) $t = 367$, (c) $t = 490$, (d) $t = 688$, (e) $t = 783$, and (f) $t = 800$. Parameters are chosen as the same as those in Fig. 2.

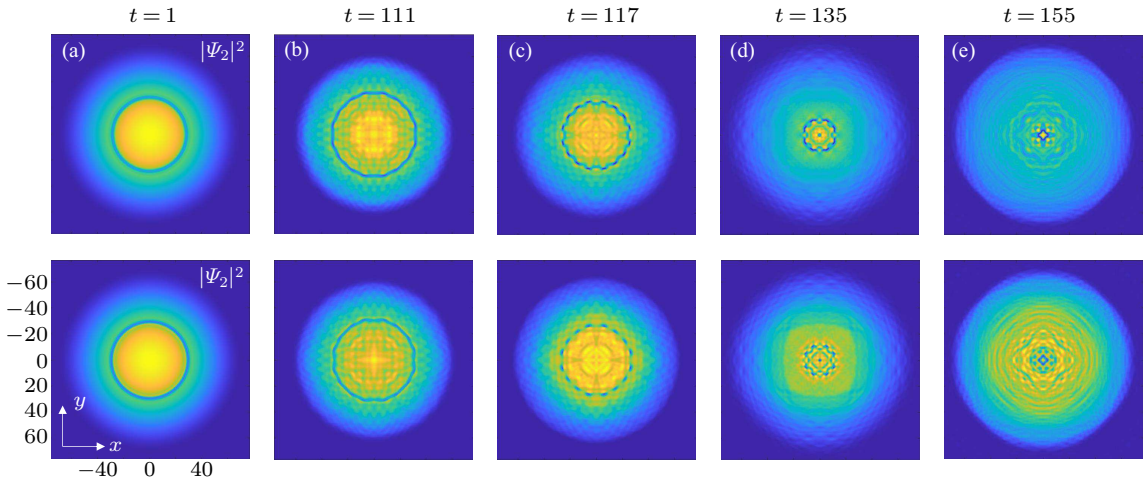


Fig. 4. The typical time evolution diagram of the gray RDSs with an initial depth of $\cos\phi_1(0) = \cos\phi_2(0) = 0.75$. (a) $t = 1$, (b) $t = 111$, (c) $t = 117$, (d) $t = 135$, and (e) $t = 155$. The top row is for component 1, while the bottom row is for component 2. The eccentricity is $e_c = 0$, the initial radii are $R_{10} = 27.9$ and $R_{20} = 28.9$, the modulation amplitude is $k = 0.02$, the modulation frequency is $\omega = 0.028$, and the aspect ratio of the harmonic trap is $\Omega = \omega = 0.028$. The intra-component Rydberg interaction in the components is $A_{11} = A_{22} = A = 0.08$. The field of view is 150×150 in dimensionless units.

Figures 4 and 5 exhibit the typical time evolution of the gray RDSs and vortices formed after these collapse for the initial depth to $\cos\phi_1(0) = \cos\phi_2(0) = 0.75$. The initial gray RDSs oscillates along the radial direction until the snake instability sets in, as shown in Fig. 4(b) for $t = 111$. Afterwards, the deformed gray soliton decays into a necklace-like structure with 16 pairs of vortices arranged in a ring, as shown in Fig. 4(c) at $t = 117$. The necklace vortex array maintains its radially inward contraction dynamics, replicating the behavior observed in the previous case. This convergent motion induces successive mergers between adjacent vortices, with the system's topological configuration undergoing a remarkable transformation. The coalescence process progressively reduces the number of vortex pairs from the initial 16 to 8,

accompanied by the emergence of a defined petal shaped morphology, as shown in Fig. 4(d) for $t = 135$. The convergent motion is held until a loop with a smaller radius is created, as shown in Fig. 4(e). The mini RDS collapse rapidly into new lump solitons that return outward subsequently along the + shape direction, as shown in Fig. 5(a) for $t = 178$. During the motion towards the periphery of the condensate, the lump solitons transform into vortex pairs, which split at into vortices and antivortices moving in opposite directions, subsequently recombining the quartets of new vortex pairs along the x-direction that propagates back toward the center, as shown in Figs. 5(b)–5(e). These vortices will repeat similar oscillatory motion including periodic splitting, recombination, and rebound until annihilation occurs due to energy dissipation or topological charge cancellation.

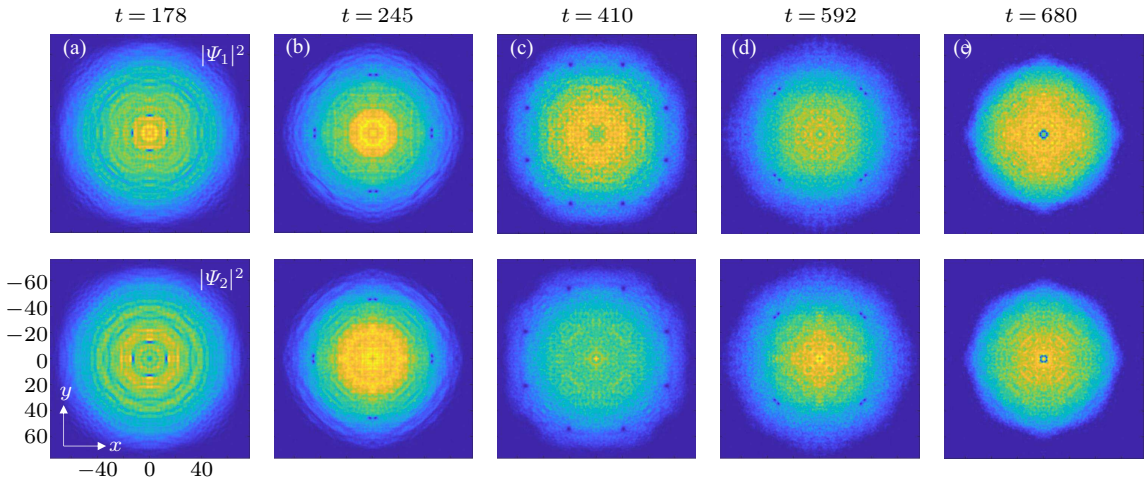


Fig. 5. The typical time evolution diagram of the gray RDSs with an initial depth of $\cos\phi_1(0) = \cos\phi_2(0) = 0.75$. (a) $t = 178$, (b) $t = 245$, (c) $t = 410$, (d) $t = 592$, and (e) $t = 680$. Parameters are chosen as the same as those in Fig. 4.

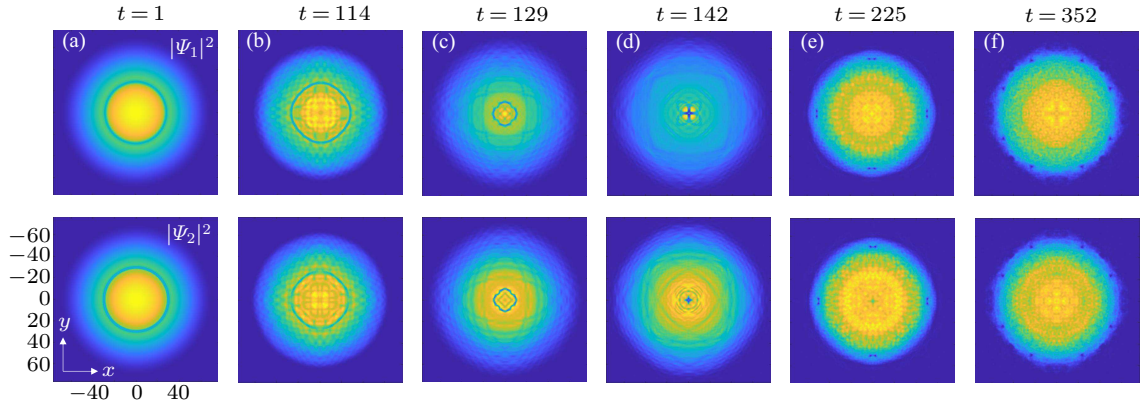


Fig. 6. The typical time evolution diagram of the deep gray RDSs with an initial depth of $\cos\phi_1(0) = \cos\phi_2(0) = 0.63$. (a) $t = 1$, (b) $t = 114$, (c) $t = 129$, (d) $t = 142$, (e) $t = 225$, and (f) $t = 352$. The top row is for component 1, while the bottom row is for component 2. The eccentricity is $e_c = 0$, the initial radii are $R_{10} = 27.9$ and $R_{20} = 28.9$, the modulation amplitude is $k = 0.02$, the modulation frequency is $\omega = 0.028$, and the aspect ratio of the harmonic trap is $\Omega = \omega = 0.028$. The intra-component Rydberg interaction in the components is $A_{11} = A_{22} = A = 0.08$. The field of view is 150×150 in dimensionless units.

Finally, we continuously reduced the initial depth of the gray RDSs, thus theirs nonlinear localization properties are significantly weakened, rendering the soliton increasingly vulnerable to snake instability. Our numerical results confirm this that the collapse of shallower gray RDSs lead to a obvious reduction in the number of formed vortices. Even when the initial depth of gray RDSs is reduced to $\cos\phi_1(0) = \cos\phi_2(0) = 0.63$, it still undergoes distortion and decays into four pairs of vortex, as shown in Fig. 6. The dynamical behavior of the quartets of pairs is similar to the process described in Fig. 5. It is worthy mentioning that quadruple vortex pairs are formed if the initial depth of gray RDSs exceeds a critical threshold of $\cos\phi(0) > 0.54$ with periodically modulated Rydberg-dressed interaction systems. This critical depth is slightly lower than the previously reported values for generating typical topological defect.[30] The findings provide new insights for manipulating gray solitons or vortices in experiments.

We also provide an experimental protocol for observing the above dynamical phenomena. The physical system considered here can be realized by a two-component system of BECs, e.g., in the $|F = 1, m_f = -1\rangle$ and $|F = 1, m_f = 0\rangle$ spin states of ^{87}Rb. The Rydberg interaction can be realized by using the Rydberg dressing technique,[58–60] and its strength can be changed within a wide range by tuning the two-photon

Rabi frequency and detuning.[29] Consequently, the parameter space considered in this work is within the reach of the current experimental technology.

4. Conclusion

In summary, we have investigated the dynamics of gray RDSs in a binary BECs with periodically modulated Rydberg interactions. It is found that the lifetime of gray RDSs with periodically modulated soft-core interactions significantly depends on their initial depth. Specifically, shallower initial depths lead to longer lifetimes when exceeding a critical depth threshold of $\cos\phi(0) > 0.54$. And the deeper the initial depth of the gray RDSs generate the more vortex pairs after collapse, which dynamic behavior becomes more complex. These depth-dependent topological transformations open new perspectives for quantum manipulation. We hope that these results can serve as a valuable reference for further research on the dynamics of gray RDSs.

Acknowledgements

Project supported by the National Natural Science Foundation of China (Grant Nos. 12175129, 12475004, 12175027, and 12005125), the Key Research Program of Frontier Sciences of the Chinese Academy of Sciences (Grant No. ZDBS-LY7016), the Shaanxi Fundamental Science Research Project for Mathematics and Physics (Grant No. 22JSY034), the Key Research and Development Projects of Shaanxi Province, China (Grant No. 2024GX-YBXM-564), the Scientific Research Program Funded by Shaanxi Provincial Education Department (Grant No. 23JP020), and the Youth Innovation Team of Shaanxi Universities.

References

[1] Bloch I, Dalibard J and Zwerger W 2008 *Rev. Mod. Phys.* **80** 885
[2] Niu Z X and Gao C 2024 *Chin. Phys. B* **33** 020314
[3] Lukin M D, Fleischhauer M, Cote R, Duan L M, Jaksch D, Cirac J I and Zoller P 2001 *Phys. Rev. Lett.* **87** 037901
[4] Guo H, Wang Y J, Wang L X and Zhang X F 2020 *Acta Phys. Sin.* **69** 010302 (in Chinese)
[5] Heidemann R, Krohn U, Bendkowsky V, Butscher B, Löw R and Pfau T 2008 *Phys. Rev. Lett.* **100** 033601
[6] Xu D H and Lou S Y 2020 *Acta Phys. Sin.* **69** 014208 (in Chinese)
[7] Fan S T, Zhang Y Y, Yan L L, Guo W G, Zhang S G and Jiang H F 2019 *Chin. Phys. B* **28** 064204
[8] Henkel N, Cinti F, Jain P and Pohl T 2012 *Phys. Rev. Lett.* **108** 265301
[9] Strecker K E, Partridge G B, Truscott A G and Hulet R G 2002 *Nature* **417** 150
[10] Niu Z X and Gao C 2024 *Chin. Phys. B* **33** 020314
[11] Shou Q, Liu D W, Zhang X, Hu W and Guo Q 2014 *Chin. Phys. B* **23** 084204
[12] Dalfovo F, Giorgini S, Pitaevskii L P and Stringari S 1999 *Rev. Mod. Phys.* **71** 463
[13] Spielman I B 2013 *Physics Today* **66** 47
[14] Toikka L A and Suominen K A 2013 *Phys. Rev. A* **87** 043601
[15] Nistazakis H E, Frantzeskakis D J, Malomed B A and Kevrekidis P G 2001 *Phys. Lett. A* **285** 157
[16] Stockhofe J, Kevrekidis P G, Frantzeskakis D J and Schmelcher P 2011 *J. Phys. B: At. Mol. Opt. Phys.* **44** 191003
[17] Katsimiga G C, Mistakidis S I, Koutentakis G M, Kevrekidis P G and Schmelcher P 2017 *New J. Phys.* **19** 123012
[18] Leda J, Miyakawa T and Wadati M 2004 *Phys. Rev. Lett.* **93** 194102
[19] Fialko O, Brand J and Zülicke U 2012 *Phys. Rev. A* **85** 051605
[20] Wang L X, Dai C Q, Wen L, Liu T, Jiang H F, Saito H, Zhang S G and Zhang X F 2018 *Phys. Rev. A* **97** 063607
[21] Barredo D, De Léséleuc S, Lienhard V and Browaeys A 2016 *Science* **354** 1021
[22] Zhong Y, Triki H and Zhou Q 2024 *Chin. Phys. Lett.* **41** 070501
[23] Pupillo G, Micheli A, Boninsegni M and Zoller P 2010 *Phys. Rev. Lett.* **104** 223002
[24] Saffman M, Walker T G and Mølmer K 2010 *Phys. Rev. Lett.* **82** 2313
[25] Kanamoto R, Saito H and Ueda M 2005 *Phys. Rev. Lett.* **94** 090404
[26] Zeiher J, Van Bijnen, R, Schauß P, Hild S, Choi J Y, Pohl T, Bloch I and Gross C 2016 *Chaos, Solitons and Fractals* **12** 1095
[27] Wright K C, Blakestad R B, Lobb C J, Phillips C J, Phillips W D and Campbell G K 2013 *Phys. Rev. Lett.* **110** 025302
[28] Henkel N, Nath R and Pohl T 2010 *Phys. Rev. Lett.* **104** 195302
[29] Balewski J B, Krupp A T, Gaj A, Hofferberth S, Löw R and Pfau T 2014 *New J. Phys.* **16** 063012
[30] Theocharis G, Frantzeskakis D J, Kevrekidis P G, Malomed B A and Kivshar Y S 2003 *Phys. Rev. Lett.* **90** 120403
[31] Abdullaev F K, Gammal A, Malomed B A and Tomio L 2014 *J. Phys. B: At. Mol. Opt. Phys.* **47** 075301
[32] Ho T L 2001 *Phys. Rev. Lett.* **87** 060403
[33] Nguyen J H V, Dyke P, Luo D, Malomed B A and Hulet R G 2014 *Nat. Phys.* **10** 918
[34] Becker C, Stellmer S, Soltan-Panahi P, Dörscher S, Baumert M, Richter E M, Kronjäger J, Bongs K and Sengstock K 2008 *Nat. Phys.* **4** 496
[35] Dutton Z, Budde M, Slowe C and Hau L V 2001 *Science* **293** 663
[36] Zhong Y, Triki H and Zhou Q 2024 *Chin. Phys. Lett.* **41** 070501
[37] Liu X X, Pu H, Xiong B, Liu W M and Gong J B 2009 *Phys. Rev. A* **79** 013423
[38] He Z M, Wen L, Wang Y J, Chen G P, Tan R B, Dai C Q and Zhang X F 2019 *Phys. Rev. E* **99** 062216
[39] Carr L D and Brand J 2004 *Phys. Rev. Lett.* **92** 040401
[40] Öhberg P and Santos L 2001 *Phys. Rev. Lett.* **86** 2918
[41] Denschlag J, Simsarian J E, Feder D L, Clark C W, Collins L A, Cubizolles J, Deng L, Hagley E W, Helmerson K, Reinhardt W P, Rolston S L, Schneider B I and Phillips W D 2000 *Science* **287** 97
[42] Böttcher F, Schmidt J N, Hertkorn J, Ng K S, Graham S D, Guo M and Pfau T 2020 *Rep. Prog. Phys.* **84** 012403
[43] Han W, Zhang X F, Song S W, Saito H, Zhang W, Liu W M and Zhang S G 2016 *Phys. Rev. A* **94** 033629
[44] Kim E and Chan M H W 2004 *Nature* **427** 225
[45] Heidemann R, Krohn U, Bendkowsky V, Butscher B, Löw R and Pfau T 2008 *Phys. Rev. Lett.* **100** 033601
[46] Ebert M, Kwon M, Walker T G and Saffman M 2015 *Phys. Rev. Lett.* **115** 093601
[47] Kevrekidis P G, Frantzeskakis D J and Carretero-González R 2015 *The defocusing nonlinear Schrödinger equation: from dark solitons to vortices and vortex rings* (Oxford: Society for Industrial and Applied Mathematics) p. 76
[48] Frantzeskakis D J 2017 *J. Phys. A: Math. Theor.* **43** 213001
[49] Zhang X F, Hu X H, Liu X X and Liu W M 2009 *Phys. Rev. A* **79** 033630
[50] Zhang X F, Wen L, Wang L X, Chen G P, Tan R B and Saito H 2022 *Phys. Rev. A* **105** 033306
[51] Petrov D S, Holzmann M and Shlyapnikov G V 2000 *Phys. Rev. Lett.* **84** 2551
[52] Petrov D S and Shlyapnikov G V 2001 *Phys. Rev. A* **64** 012706
[53] Bao W, Jaksch D and Markowich P A 2003 *J. Comput. Phys.* **187** 318
[54] Kasamatsu K, Tsubota M and Ueda M 2003 *Phys. Rev. A* **67** 033610
[55] Cavina V, Soret A, Aslyamov T, Ptaszyński K and Esposito M 2024 *Phys. Rev. Lett.* **133** 130401
[56] Wang L X, He Q L, Zhai H H, Liu H, Chen S L, Yang X Y and Zhang X F 2024 *Ann. Phys.* **465** 169683
[57] Wang L X, Liu H, Yang H L, Chen S L, Tu P, Wen L, Yang X Y and Zhang X F 2024 *Ann. Phys.* **181** 114664
[58] Hall D S, Matthews M R, Ensher J R, Wieman C E and Cornell E A 1998 *Phys. Rev. Lett.* **81** 1539
[59] Hu X H, Zhang X F, Zhao D, Luo H G and Liu W M 2009 *Phys. Rev. A* **79** 023619
[60] Burger S, Bongs K, Dettmer S, Ertmer W, Sengstock K, Sanpera A, Shlyapnikov G V and Lewenstein M 1999 *Phys. Rev. Lett.* **83** 5198